Sigma J Eng Nat Sci, Vol. 44, No. 1, pp. 262–272, February, 2026

Sigma Journal of Engineering and Natural Sciences
Web page info: https://sigma.yildiz.edu.tr
DOI: 10.14744/sigma.2025.00060

Research Article

An exact analysis of chemical reaction and porosity effects for mixed convective magnetohydrodynamics Casson fluid

Nur Fatihah MOD OMAR[1], Zulkhibri ISMAIL[1,*], Rahimah JUSOH[1], Muhammad Azrin AHMAD[1], Ahmad Qushairi MOHAMAD[2]

[1]Centre for Mathematical Sciences, Universiti Malaysia Pahang Al-Sultan Abdullah, Lebuhraya Persiaran Tun Khalil Yaakob, Gambang, Pahang, 26300, Malaysia
[2]Department of Mathematical Sciences, Faculty of Science, Universiti Teknologi Malaysia, Johor Bahru, Johor, 81310, Malaysia

ARTICLE INFO

Article history
Received: 04 August 2024
Revised: 17 October 2024
Accepted: 13 January 2025

Keywords:
Accelerated Plate; Casson Fluid; Chemical Reaction; Magnetohydrodynamic; Radiation

ABSTRACT

In this research, we explore the Casson fluid flow under mixed convection in a plate undergoing acceleration within a porous medium, considering the effects of chemical reaction and magnetisation. The investigation encompasses heat and mass transfer characteristics, incorporating thermal radiation and chemical reactions. Inspired by the previous studies of the chemical reaction and porosity of magnetohydrodynamic Casson fluid, the focus of this research revolves around the Casson parameter with convective double diffusion flows with magnetohydrodynamics (MHD) over a plate undergoing acceleration within a porous medium, considering the occurrence of a radiative chemical reaction. Ordinary differential equations are transformed from the governing partial differential equations through appropriate non-dimensional variables to facilitate mathematical analysis. Subsequently, the Laplace transform method is utilised to get the solution for the resulting non-dimensional ordinary differential equations system. The study provides graphical representations illustrating the behaviour of various physical parameters. The trend reveals that the rising Casson parameter will descend the fluid velocity, primarily attributed to the elevated fluid viscosity. Notably, the Casson parameter has no impact as the fluid approaches the centre between the bounding surfaces. Additionally, it is seen that a higher Casson parameter results in behaviour resembling that of a Newtonian fluid. On top of that, the velocity increases significantly for larger chemical reaction coefficient values. Finally, it is noticed that velocity tends to decrease as the porosity parameter decreases and the magnetic field strength increases.

Cite this article as: Mod Omar NF, İsmail Z, Jusoh R, Ahmad MA, Mohamad AQ. An exact analysis of chemical reaction and porosity effects for mixed convective magnetohydrodynamics Casson fluid. Sigma J Eng Nat Sci 2026;44(1):262–272.

***Corresponding author.**
*E-mail address: zulkhibri@umpsa.edu.my

This paper was recommended for publication in revised form by Editor-in-Chief Ahmet Selim Dalkilic

INTRODUCTION

A chemical reaction is a transformative process in which one group of chemical substances changes into another. Additionally, chemical reactions often occur between a fluid and a foreign mass. Typically, these categories are divided into two primary categories; homogeneous and heterogeneous chemical reactions, contingent on whether they transpire at an interface or within a volume comprising a single phase. The scrutiny of flows of mass transfer involving chemical reactions has proven highly valuable in various chemical and hydrometallurgical industries. This encompasses applications like catalytic chemical reactors, food processing, processes involving either endothermic or exothermic chemical reactions, and the manufacturing of glassware and ceramics [1]. The extensive application of mass transport with activation energy, as necessitated by the above, has captured the interest of researchers. The concept of activation energy was introduced by Arrhenius in 1889, representing the least amount of energy needed for particles to engage in a chemical reaction. They conferred that this energy could manifest as kinetic or potential energy, and without it, the transformation of reactants into products cannot occur [2]. Research has been carried out to examine double diffusions in the context of the Casson fluid flow, with magnetohydrodynamic over a wedge with the inclusion of thermal radiation and chemical reaction. The concentration of Casson fluid decreases due to the chemical reaction parameter actively rising. This is because the chemical reaction hinders the fluid's momentum [3]. Recently, Sene [4] discussed a solution method for the model of fractional Casson fluid, adapting the chemical reaction and heat generation impact. It shows that the Casson fluid parameter influences the boundary layer thickness and induces the velocity to rise.

Casson fluid stands out as one of the ultimate renowned non-Newtonian fluids. Casson introduced this substance as a crucial element of pseudoplastic fluids in 1959. The Casson fluid model offers two significant strengths; firstly, the derivation is from liquid kinetic theory rather than an empirical correlation, and secondly, it transforms to a Newtonian nature at certain shear rates [5]. Casson fluid behaves like a solid when the yield stress exceeds the shear stress, but it flows like a liquid when the yield stress is lower than the shear stress [6]. Moreover, it is also appropriate for heating and cooling processes due to their effective influence on the rate of energy transfer [7]. In 2018, Hussanan et al. [8] considered unsteady natural convection of a nanofluid flow based on sodium alginate viscoplastic Casson fluid over a vertical plate. By implying uniform free stream velocity as well as temperature, it is resolved by applying the Runge–Kutta numerical method in combination with a shooting technique. The conclusion discloses that the velocity field diminishes when the Casson parameter elevates. Aman et al. [9] explored using Caputo time-fractional models towards MHD Casson fluid flow. Fractional calculus is an intriguing subject due to its applications in Mathematics, Applied Mathematics, and Fluid Dynamics. Moreover, Akhil and Patel [10] enticed the influence of heat generation and non-linear radiation on the mixed convection MHD Casson fluid flow. It can be inferred that the Casson fluid parameter tends to lower both skin friction and concentration profiles. Subsequently, by means of an accelerated plate, Shahrim et al. [11] investigated a fractional convection problem involving Casson fluid. As a point of reference, the use of fractional derivatives to characterise the physical properties of non-Newtonian fluid flow over accelerated plate remains uncommon. Their findings indicated that the velocity would escalate by ascending values of time, t and Grashof number, Gr. Conversely, a decrease in the Prandtl number, Pr and Casson fluid parameter reduced velocity.

Magnetohydrodynamics (MHD) illustrates the behaviour of fluids with high conductivity in the occurrence of magnetisation. These MHD flows play a crucial role in diverse applications, including MHD energy generators, cancer treatment, biomedical flow control, magneto-fluid rotary blood pumping, drug targeting through MHD, materials processing, separation devices, and bio-micro-fluidic devices utilizing MHD [12]. The core principle of magnetohydrodynamics (MHD) is that a magnetic field can generate flows in a conductive fluid in motion, resulting in fluid polarization and altering the magnetic field. The equations governing MHD combine the Navier–Stokes equations of fluid dynamics with Maxwell's equations of electromagnetism. Examples of such magneto-fluids include plasmas, liquid metals, salt water, and electrolytes [13]. Given its diverse technological and engineering applications, a comprehensive understanding and exploration of Magnetohydrodynamics (MHD) flow is crucial. The major goal of MHD fundamentals is to steer the flow field in a predetermined specific direction by changing the boundary layer development. Consequently, the implementation of MHD appears to be a further adaptable and dependable approach for modifying flow kinematics. In the realms of pharmaceuticals and environmental science, MHD plays a pivotal part in biomedical engineering and fluid dynamics applications. Chemical engineering employs MHD for both purification and filtration objectives [14]. Ismail et al. [15] undertook a study to investigate the impact of magnetohydrodynamics (MHD) along with radiation under ramped wall temperature conditions on natural convection through a porous medium past an infinitely inclined plate. They employed the Laplace transform method in their analysis. Furthermore, Prasad [16] discussed the thermal and species concentration characteristics of MHD Casson fluid along a vertical sheet. On top of that, Jagadesh et al. [17] have performed an analysis of dissipative heat transfer and peristaltic pumping in the context of MHD Casson fluid flow within an inclined channel. Their findings indicated that incremental in both magnetisation and Casson parameter led to an elevation in the heat transfer rate. Recently, J

Raza et al. studied Casson nanofluid past a stretching sheet and discovered that an increase in the magnetic parameter amplifies the Brownian motion of fluid particles, leading to a gradual rise in the fluid's temperature [18].

Presently, numerous researchers have examined the effects of fluid thermal radiation on the properties of heat transport over extended surfaces. The process of heat transfer is significant in the implementation of photochemical reactors and solar power technology. The term thermal radiation refers to the emission of electromagnetic waves by a substance, leading to an increase in its internal energy and resulting in warming [19]. Kataria and Patel [20] successfully derived the solution analytically for the flow of an oscillating plate through an MHD Casson fluid, in addition to radiative chemical reaction parameters. [21] examines heat and mass transfer in a magnetohydrodynamic flow over a moving vertical plate with convective boundary conditions under the influence of thermal radiation. Increased values of the radiation parameter promote conduction over radiation, thereby reducing the thermal boundary layer thickness. Besides, Omar et al. [22] studied the influence of radiation and Magnetohydrodynamic of Casson Fluid over a plate undergoing acceleration. It was discovered that thermal radiation increases with a temperature rise.

Khan [23] investigated the unsteady squeezing flow of MHD Casson fluid flowing via a porous medium. The term porous medium is recognised as a substance containing fluid-filled pores and is consistently defined by attributes like porosity and permeability. Porosity determines the volume of fluid the material can retain, while permeability quantifies the fluid's ability to traverse through it. Diverse applications encompass chemical reactors, groundwater hydrology, drainage, seepage, irrigation, and the extraction of crude oil from reservoir rock pores. Several intriguing findings are present within [24–26].

Inspired by the aforementioned research, the focus of this research revolves around the Casson parameter with convective double diffusion flows with magnetohydrodynamics over a plate undergoing acceleration within a porous medium, considering the occurrence of the radiative chemical reaction. Limiting cases are conducted to verify consistency with previous findings. These analytical solutions can help scientists and engineers verify the accuracy of complex model solutions derived from numerical schemes. This research work can later be extended by using different fluids. Additionally, the proposed mathematical model is anticipated to serve as a reference for researchers in academia, engineering, and industry, facilitating further analysis of flow characteristics, heat transfer, and mass transfer performance of such fluids.

MATHEMATICAL FORMULATION

The research intends to obtain solutions in the presence of porous medium, magnetohydrodynamics and chemical reaction as well as radiation. The focus is on the context of an unsteady Casson fluid flowing in a state of the accelerated plate, positioned at the flow being restrained to $x > 0$, where x denotes the coordinate measurement in the direction perpendicular to the surface. At the start, at the time $t = 0$ the plate and fluid are at rest, exhibiting a uniform concentration and temperature. Then, as $t > 0$, the plate undergoes acceleration with a velocity $u' = At$ and concurrently, the temperature of the plate is increased to T'_w while the concentration is elevated to T'_w.

The dimensional momentum, energy, and concentration equations that govern the flow are as follows:

$$\rho \frac{\partial u'}{\partial t'} = \mu \left(1+\frac{1}{\gamma}\right)\frac{\partial^2 u'}{\partial x'^2} + \rho g \beta_T \left(T'-T'_\infty\right) + \rho g \beta_C \left(C-C'_\infty\right) - \sigma B_0^2 u' - \frac{\mu \varphi}{K} u' \tag{1}$$

$$\rho c_p \frac{\partial T'}{\partial t'} = k \frac{\partial^2 T'}{\partial x'^2} - \frac{\partial q'_r}{\partial x'} \tag{2}$$

$$\rho c_p \frac{\partial C'}{\partial t'} = D \frac{\partial^2 C'}{\partial x'^2} - Kr'(C'-C'_\infty) \tag{3}$$

In the given context, γ represents the parameter of Casson fluid, u' denotes fluid in the x- direction, t depicts the variable of time, T' corresponds to the temperature of the fluid near the plate, whereas T'_∞ signifies the plate temperature, C' represents concentration, ρ stands for fluid density, μ represents dynamic viscosity, g signifies acceleration due to gravity, β represents the thermal expansion coefficient, B_0 indicates external magnetic field, σ is the electrical conductivity, φ refers to the porosity, k represents thermal conductivity, K denotes permeability, c_p refers to specific heat at constant pressure, q_r signifies radiative heat flux, D refers to mass diffusion and Kr indicates chemical reaction alongside the initial value and boundary conditions:

$$\begin{aligned} &u'(x',0) = 0; \quad u'(0,t') = At; \quad u'(\infty,t') = 0; \\ &T'(x',0) = T'_\infty; \quad T'(0,t) = T'_w; \quad T'(\infty,t) = T'_\infty, \\ &C'(x',0) = C'_\infty; \quad C'(0,t) = C'_w; \quad C'(\infty,t) = C'_\infty, \end{aligned} \tag{4}$$

MATHEMATICAL SOLUTION

Through the introduction of dimensionless variables:

$$u = \frac{u'}{(\nu A)^{\frac{1}{3}}}; \; t = \frac{t' A^{\frac{2}{3}}}{\nu^{\frac{1}{3}}}; \; x = \frac{x' A^{\frac{1}{3}}}{\nu^{\frac{2}{3}}}; \; T = \frac{T'-T'_\infty}{T'_w - T'_\infty}; \; C = \frac{C'-C'_\infty}{C'_w - C'_\infty} \tag{5}$$

The dimensionless representation of equations (1) - (3),

$$\frac{\partial u}{\partial t} = A\frac{\partial^2 u}{\partial x^2} + GrT - Bu + GcC \tag{6}$$

$$\lambda \frac{\partial T}{\partial t} = \frac{\partial^2 T}{\partial x^2} \tag{7}$$

$$\frac{\partial C}{\partial t} = \frac{1}{Sc}\frac{\partial^2 C}{\partial x^2} - KrC \tag{8}$$

The method of Laplace transform is employed for equations (6) - (8),

$$\frac{d^2\overline{U}}{dx^2} - \frac{(s+B)}{A}\overline{U} = -P\overline{T} - Q\overline{C} \tag{9}$$

$$\frac{d^2\overline{T}}{dx^2} - \lambda s\overline{T} = 0 \tag{10}$$

$$\frac{d^2\overline{C}}{dx^2} - \overline{C}(ScKr + Scs) = 0 \tag{11}$$

The transformed equations are,

$$\overline{U} = \left(\frac{1-e^{-s}}{s^2} - \frac{a1}{s(s-a2)} - \frac{a3}{s(s-a4)}\right)e^{-x\sqrt{\frac{(s+B)}{A}}} + \frac{a1}{s(s-a2)}e^{-x\sqrt{\lambda s}} + \frac{a3}{s(s-a4)}e^{-x\sqrt{Sc}\sqrt{s+Kr}} \tag{12}$$

$$\overline{T} = \frac{1}{s}e^{-x\sqrt{\lambda s}} \tag{13}$$

$$\overline{C} = \frac{1}{s}e^{-x\sqrt{Sc}\sqrt{(s+Kr)}} \tag{14}$$

and the parameters utilised in this study are as follows:

$$Gr = \frac{g\beta(T_w - T_\infty)}{A};\quad A = 1 + \frac{1}{\gamma};\quad B = M + \frac{1}{K};\quad \lambda = \frac{\Pr}{1+N};\quad P = \frac{Gr}{A};$$

$$Gc = \frac{g\beta(C_w - C_\infty)}{A};\quad Q = \frac{Gc}{A};\quad M = \frac{\sigma B_0^{2*} v^{\frac{1}{3}}}{\rho A^{\frac{2}{3}}};\quad N = \frac{16\sigma^* T_\infty'^3}{3kk^*};\quad \Pr = \frac{\mu c_p}{k}.$$

Solutions for equations (12), (13), and (14) are subsequently obtained by inversing the method of Laplace transform:

$$T(x,t) = erfc\frac{x\sqrt{\lambda}}{2\sqrt{t}}$$

$$C(x,t) = \begin{pmatrix} \frac{1}{2}((e^{x\sqrt{ScKr}}\, erfc\frac{x\sqrt{Sc}}{2\sqrt{t}} + \sqrt{Krt}) \\ +(e^{-x\sqrt{ScKr}}\, erfc\frac{x\sqrt{Sc}}{2\sqrt{t}} - \sqrt{Krt})) \end{pmatrix}$$

$$U0(x,t) = \begin{pmatrix} (\frac{t}{2} + \frac{x}{4}\sqrt{\frac{1}{AB}})e^{x\sqrt{\frac{B}{A}}}erfc((\frac{x}{2\sqrt{At}}) + \sqrt{Bt}) \\ +(\frac{t}{2} - \frac{x}{4}\sqrt{\frac{1}{AB}})e^{-x\sqrt{\frac{B}{A}}}erfc((\frac{x}{2\sqrt{At}}) - \sqrt{Bt}) \end{pmatrix}$$

$$U1(x,t) = \begin{pmatrix} (-\frac{a1}{a2}erfc(\frac{x\sqrt{\lambda}}{2\sqrt{t}})) + (\frac{a1}{a2}\frac{e^{a2t}}{2})((e^{x\sqrt{\lambda a2}}erfc((\frac{x\sqrt{\lambda}}{2\sqrt{t}}) + \sqrt{a2t})) \\ +(e^{-x\sqrt{\lambda a2}}erfc((\frac{x\sqrt{\lambda}}{2\sqrt{t}}) - \sqrt{a2t}) \end{pmatrix}$$

$$U2(x,t) = \begin{pmatrix} -\frac{a3}{2a4}(e^{x\sqrt{ScKr}}erfc(\frac{x\sqrt{Sc}}{2\sqrt{t}}) + \sqrt{Krt} + e^{-x\sqrt{ScKr}}erfc(\frac{x\sqrt{Sc}}{2\sqrt{t}}) \\ -\sqrt{Krt}) + \frac{a3}{a4}\frac{e^{a4t}}{2}(e^{x\sqrt{Sc(Kr+a4)}}erfc(\frac{x\sqrt{Sc}}{2\sqrt{t}}) + \sqrt{(Kr+a4)t} \\ +e^{-x\sqrt{Sc(Kr+a4)}}erfc(\frac{x\sqrt{Sc}}{2\sqrt{t}}) - \sqrt{(Kr+a4)t}) \end{pmatrix}$$

$$U3(x,t) = \begin{pmatrix} \frac{a1}{2a2}e^{x\sqrt{\frac{B}{A}}}erfc[(\frac{x}{2\sqrt{At}}) + \sqrt{Bt} + e^{-x\sqrt{\frac{B}{A}}}erfc((\frac{x}{2\sqrt{At}}) - \sqrt{Bt}) \\ -(\frac{a1}{a2}\frac{e^{a2t}}{2})((e^{x\sqrt{\frac{1}{A}(B+a2)}}erfc((\frac{x}{2\sqrt{At}}) + \sqrt{(B+a2)t}) \\ +(e^{-x\sqrt{\frac{1}{A}(B+a2)}}erfc((\frac{x}{2\sqrt{At}}) - \sqrt{(B+a2)t}) \end{pmatrix}$$

$$U4(x,t) = \begin{pmatrix} \frac{a3}{2a4}e^{x\sqrt{\frac{B}{A}}}erfc[(\frac{x}{2\sqrt{At}}) + \sqrt{Bt} + e^{-x\sqrt{\frac{B}{A}}}erfc((\frac{x}{2\sqrt{At}}) - \sqrt{Bt}) \\ -(\frac{a3}{a4}\frac{e^{a4t}}{2})((e^{x\sqrt{\frac{1}{A}(B+a4)}}erfc((\frac{x}{2\sqrt{At}}) + \sqrt{(B+a4)t}) \\ +(e^{-x\sqrt{\frac{1}{A}(B+a4)}}erfc((\frac{x}{2\sqrt{At}}) - \sqrt{(B+a4)t}) \end{pmatrix}$$

$$U(x,t) = U0(x,t) + U1(x,t) + U2(x,t) + U3(x,t) + U4(x,t)$$

with

$$a1 = \frac{aP}{A\lambda - 1};\quad a2 = \frac{B}{A\lambda - 1};\quad a3 = \frac{AQ}{ASc - 1};\quad a4 = \frac{AScKr - B}{ASc - 1}.$$

RESULTS AND DISCUSSION

This research employs an analytical approach to investigate the flow of Casson fluid under mixed convection within a porous medium, around an accelerated plate, incorporating the effects of magnetisation and chemical reactions. The analytical techniques include the Laplace transform [14,21], Fourier series [27], Homotopy Analysis Method (HAM) [20], and fractional derivative method [8,10].

The Laplace transform has certain limitations, requiring the governing equations to be linear for effective

application. While it can handle complex equations, solving them becomes challenging without computational software.

The Laplace transform belongs to a class of operations known as integral transforms. It converts a function $f(t)$ of a single variable t (interpreted as time) into a new function $F(s)$ defined in terms of another variable s, the complex frequency. The appeal of the Laplace transform lies in its ability to transform differential equations in the t, time domain into algebraic equations in the frequency domain. This simplifies the process of solving differential equations, reducing it to solving algebraic equations in the s domain. Another significant advantage is that the Laplace transform inherently incorporates initial conditions into the solution, making it especially useful for solving initial-value problems commonly encountered in studies of electrical circuits and mechanical vibrations [28 - 33]. The core idea involves transforming a constant-coefficient differential equation in $f(t)$ into a simpler algebraic equation for the Laplace-transformed function, $F(s)$ solving this algebraic equation, and then using the inverse Laplace transform to return to the original time-domain solution, $f(t)$ The precise definition of the Laplace transform and the specific properties it satisfies make this process feasible [33].

Analytical solutions offer numerous advantages. They are benchmarks for validating numerical methods and provide insights into underlying physical phenomena [34]. Additionally, they are valuable for addressing large-scale problems, such as modelling hydrocarbon reservoirs, by enabling dimensional analysis [35]. In heat conduction problems, analytical solutions act as foundational components for constructing solutions through superposition [36]. They also allow the efficient computation of exact results using concise representations for short- and large-time behaviour [37]. Furthermore, analytical solutions are essential for verifying numerical results generated by computational methods. Besides, Computational Physicists play a crucial role in resolving inconsistencies between numerical simulations and experimental data, facilitating comparisons between theory, simulations, and experimental observations [38].

It is necessitated to establish comprehensive insight into the employed model, especially when compared to previous studies. Before delving into more detailed discussions, it is essential to verify this research against previous research to confirm, its correct execution. Figure 1a provides a comparison with Shahrim et al. [11] for different Grashof numbers, Gr and Figure 1b presents the comparison for different time, t values. The results demonstrate a strong agreement between the current study and the previous one, as demonstrated by the plotted graph comparing the two. Furthermore, it has been confirmed that all the plotted graphs comply with the specified boundary conditions. Validation demonstrates a strong agreement with the studied problem. Consequently, we have confidence that the solutions obtained are accurate. The graphical interpretation and physical insight are also discussed using fixed values of $\gamma = 0.1$, $t = 1$, $N = 5$, $Pr = 7$, $M = 1$, $K = 0.2$, $Kr = 1$, $Gr = 1$, $Gc = 1$ and $Sc = 0.6$ respectively.

In Figure 2a, a concentration profile exhibits a pronounced impact from the Schmidt number. Observably, by increasing the Schmidt number, there is a deterioration in the concentration profile. This trend is attributed to the reciprocal correlation of the Schmidt number and mass diffusivity. As the value of the Schmidt number climbs, the flow of the fluid regime demonstrates lower values of mass diffusion, leading to a decrease in the distribution of concentration. In applications involving biofluid dynamics, such as blood flow, where Casson fluid models

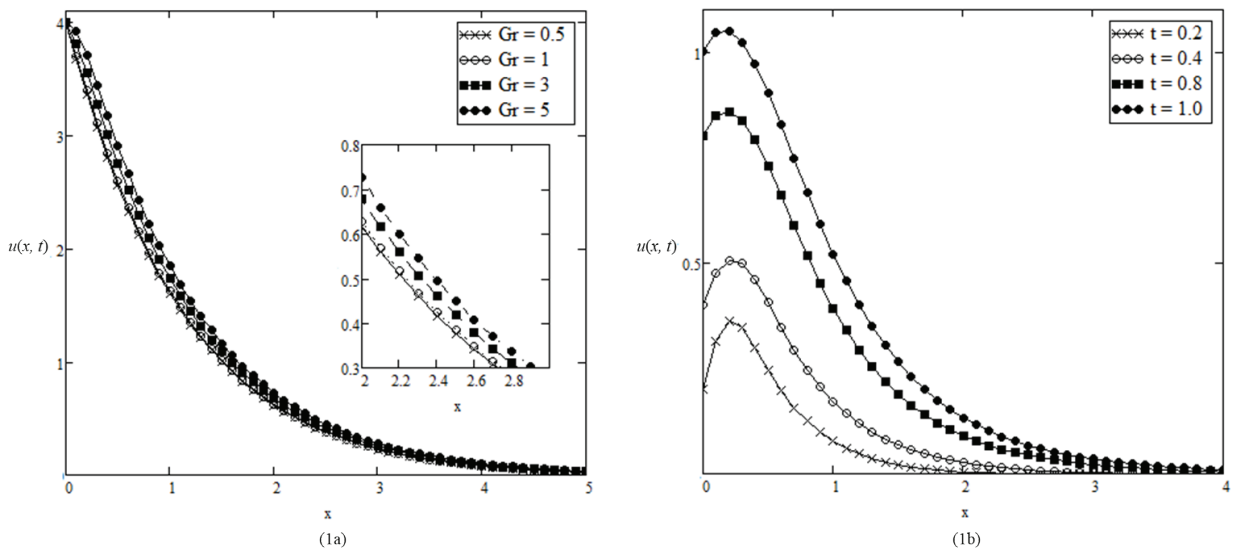

Figure 1. Validation results of Fig. 1a for different Grashof number, Gr and Fig. 1b for different time, t.

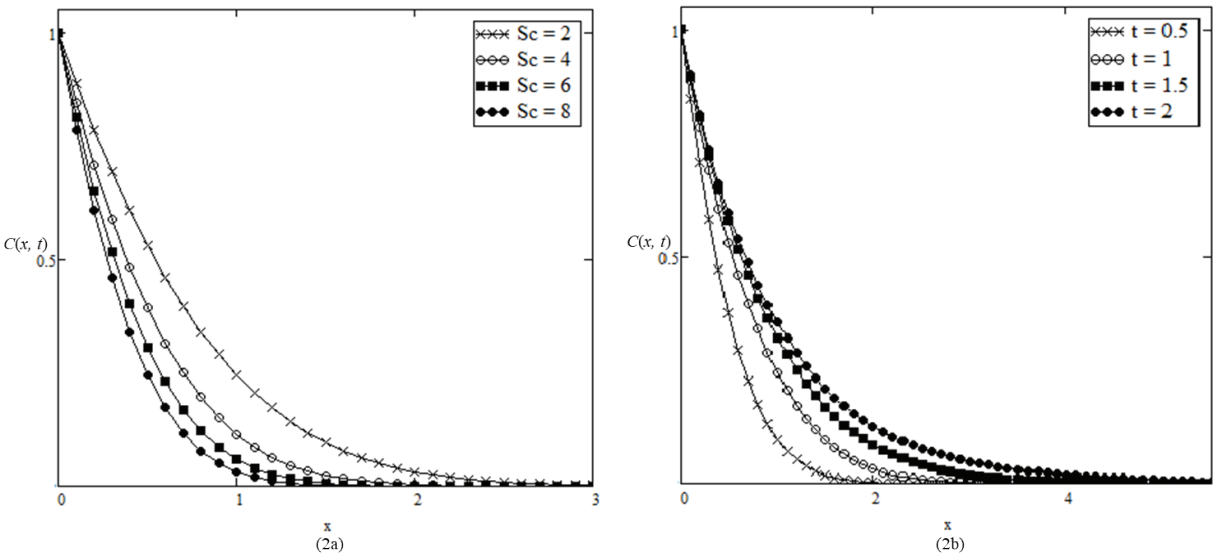

Figure 2. Concentration profiles of different Schmidt number, *Sc* (2a) and time, *t* (2b).

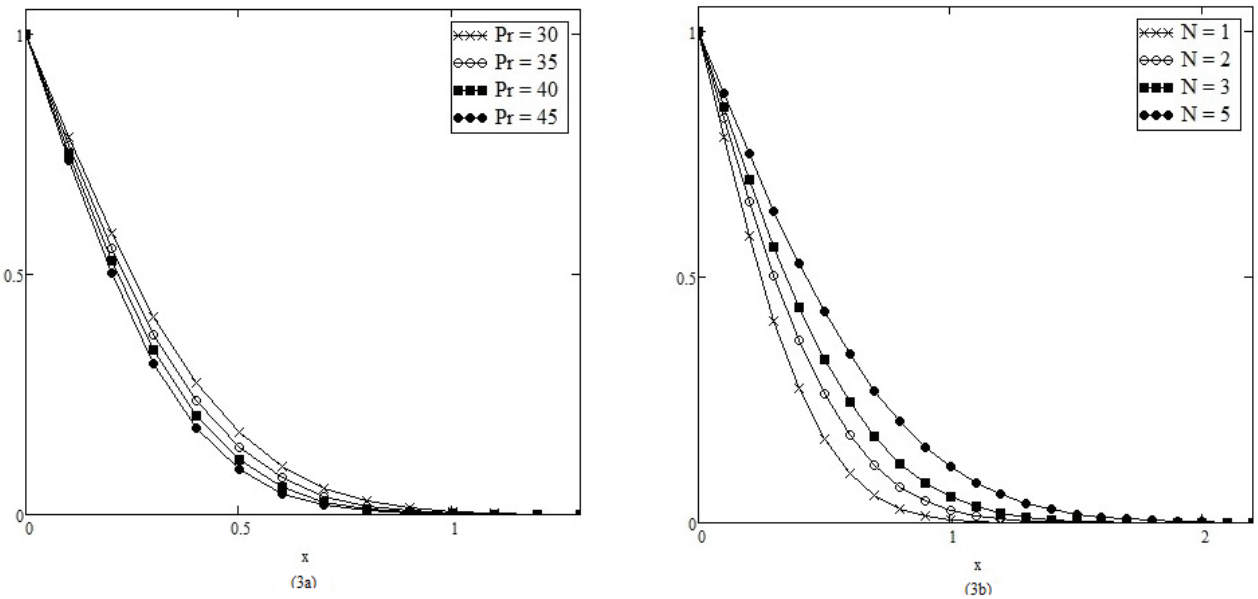

Figure 3. Temperature profiles of different Prantl number, *Pr* (3a) and radiation, *N* (3b).

are commonly employed, for example, when the Schmidt number *Sc* is high, the transport of nutrients or solutes (e.g., oxygen, pharmaceuticals) becomes less efficient due to the reduced thickness of the concentration boundary layer. This can influence the effective delivery of solutes to targeted regions in industrial or biological systems. Figure 2b illustrates the influence of time on the concentration profile, with temperature gradually increasing as time rises.

An elevation of *Pr* results in a decrement in temperature as depicted in Figure 3a. It arises from the thickness of the thermal boundary layer decreasing while the *Pr* number ascends. Figure 3b demonstrates the radiation parameter effect on the elevated temperature profile. When the radiation constraint surges, there is a rise in the thermal boundary layer thickness and temperature profile. Radiation-induced heating lowers viscosity and yield stress, enhancing fluid mobility and convective heat transfer. Increased radiation initiates steeper temperature gradients near the surface, penetrating the fluid through thermal diffusion. For instance, undertaking polymer processing in

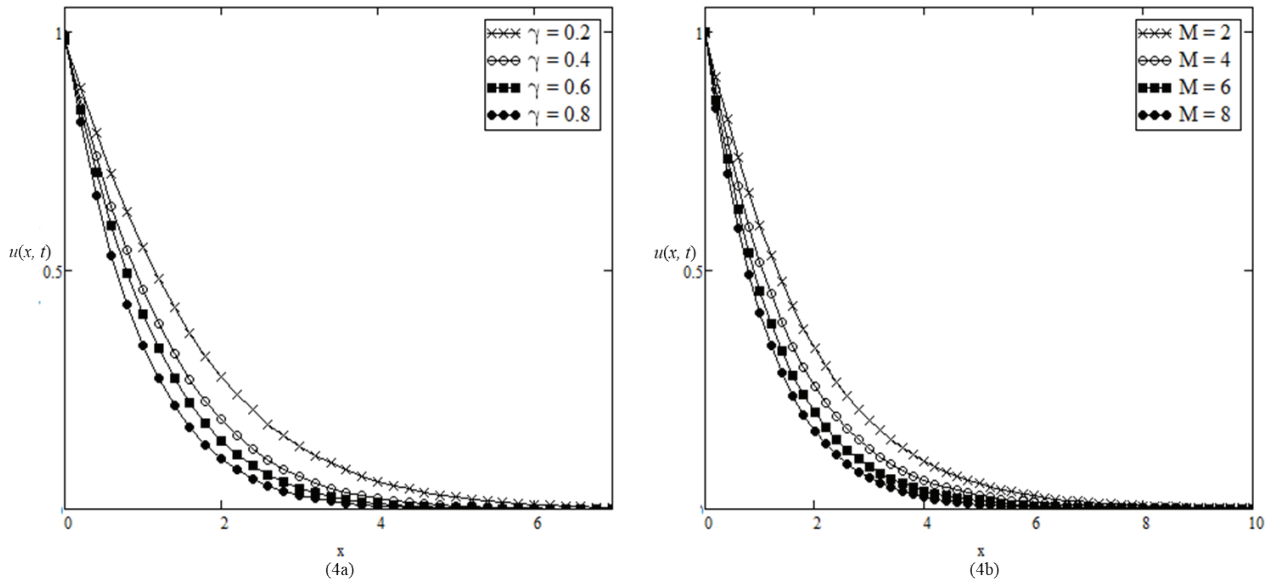

Figure 4. Velocity profiles of different Casson parameter, γ (4a) and magnetic parameter, M (4b).

industrial processes or molten metals modelled as Casson fluids, increased radiation enhances heat distribution which is essential for achieving uniform material properties. On top of that, from biomedical applications, radiative heating in capillary blood flow can lead to elevated temperatures, influencing metabolic reactions.

In Figure 4a, velocity profiles are exhibited for various Casson parameter values. The trend reveals that the rising Casson parameter will descend the fluid velocity, primarily attributed to the elevated fluid viscosity. An increased Casson parameter indicates a lower yield stress, allowing the fluid to transition to a flowing state more readily. This enhances resistance to flow and restricts the momentum transfer into the fluid, resulting in a steeper velocity gradient from the boundary to the bulk flow and a thinner boundary layer. With an increased Casson parameter, more energy is required to sustain the flow as the fluid dissipates additional energy to overcome the heightened viscous resistance. It decreases momentum transfer efficiency, confining it to a smaller region near the boundary. Notably, the Casson parameter has no impact as the fluid approaches the centre between the bounding surfaces. Additionally, it is seen that a higher Casson parameter results in behaviour resembling that of a Newtonian fluid. Consequently, boundary layer thickness velocity is higher than observed for a Newtonian fluid owing to the plasticity inherent in Casson fluid. Conversely, a decrease in the Casson parameter, associated with a rise in plasticity, results in the thickness of the boundary layer, which increases due to a simultaneous rise in the momentum boundary layer. Diving into engineering applications, in processes involving Casson fluids, such as blood flow, molten polymers, or slurries, an increase in γ results in lower flow rates and thinner boundary layers, affecting heat transfer, mixing efficiency, and pressure drop requirements. For fluids such as blood in biological systems, commonly modelled as a Casson fluid, a higher γ can indicate pathological conditions (e.g., decreased shear sensitivity due to increased plasma viscosity). This results in slower flow velocity near vessel walls and may lead to flow stagnation.

Figure 4b illustrates the impact of the magnetic field parameter M on velocity profiles. It is observed that the velocity diminishes as the magnetic field strength increases. Applying a magnetic field to a flowing, electrically conductive fluid induces an electric current in the fluid. The correlation of the induced currents and the magnetic field produces Lorentz force; referred to as a resistive force. This force acts externally in the opposite direction to the fluid flow, impeding its motion, analogous to the effect of drag force. Moreover, a rise in the magnetic parameter M will result in resistive forces, hindering the flow of the fluid, and consequently declining the velocity of the fluid.

In Figure 5a, the upshot of the chemical reaction on velocity distribution is demonstrated. It is evident that the velocity increases significantly for larger chemical reaction coefficient, Kr values. Consequently, it is established that the magnitude of the Kr coefficient plays a crucial role in shaping the velocity distribution.

Figure 5b showcases values of the porosity parameters, K for various velocity profiles, while other flow parameters are held constant. In practical terms, there is a decrease in velocity with a reduction in the porosity parameter, K. This outcome aligns with Darcy's law, which states that the presence of a porous medium descends the flow resistance, thus enhancing fluid motion. Hence, the graphical

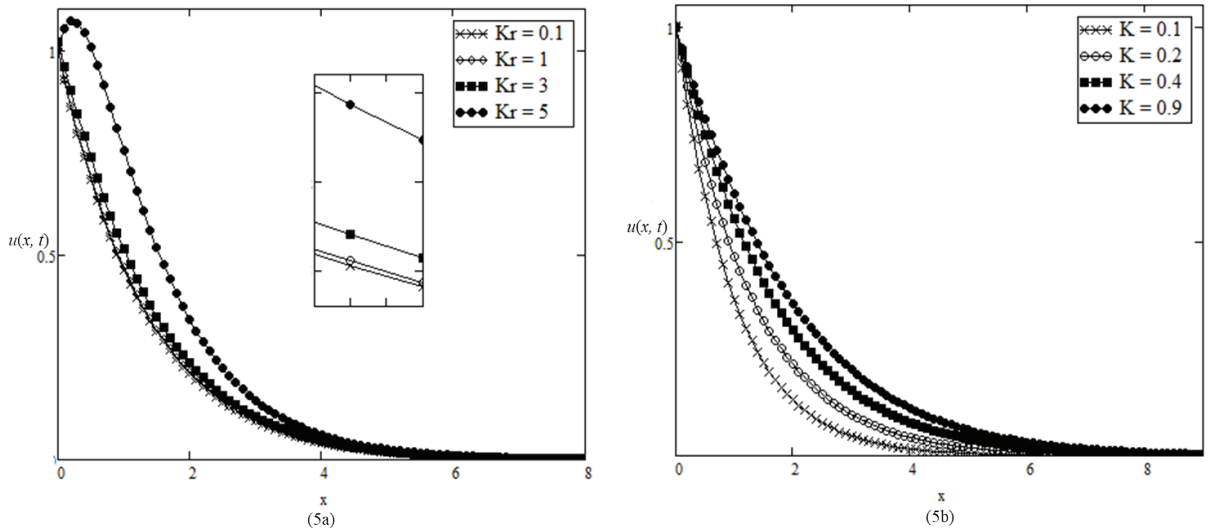

Figure 5. Velocity profiles of different chemical species parameter, *Kr* (5a) and porosity parameter, *K* (5b).

representation confirms that porosity is a pivotal factor in the current research.

Figure 6a displays the velocity profiles of the fluid for different thermal radiation values, *N*. The velocity reduces the existence of thermal radiation. This is anticipated since lower temperatures correspond to reduced radiation, leading to a decline in velocity. The fluid velocity will elevate with time, as illustrated in Figure 6b.

Figure 7a delineates the effect of the Grashof number, *Gr* on the velocity profile, symbolising the proportional thermal buoyant force's influence compared to the hydrodynamic viscous force. A steady elevation in velocity is noticed with the increasing Grashof number. This occurrence is ascribed to the intensified buoyancy force within the flow, resulting in all-in-all enhancement of fluid velocity. Figure 7b reveals the implication of the Grashof concentration number, *Gc* on the velocity profile, where the number is characterised as the ratio of species buoyant force to viscous hydrodynamic force. A rise in the *Gc* number implies the dominance of species buoyancy force relative to the force of viscous hydrodynamic, leading to a significant rise in velocity for both Casson as well as Newtonian fluids. The value of the positive Grashof number corresponds to the physical cooling of the plates. Essentially, buoyant force

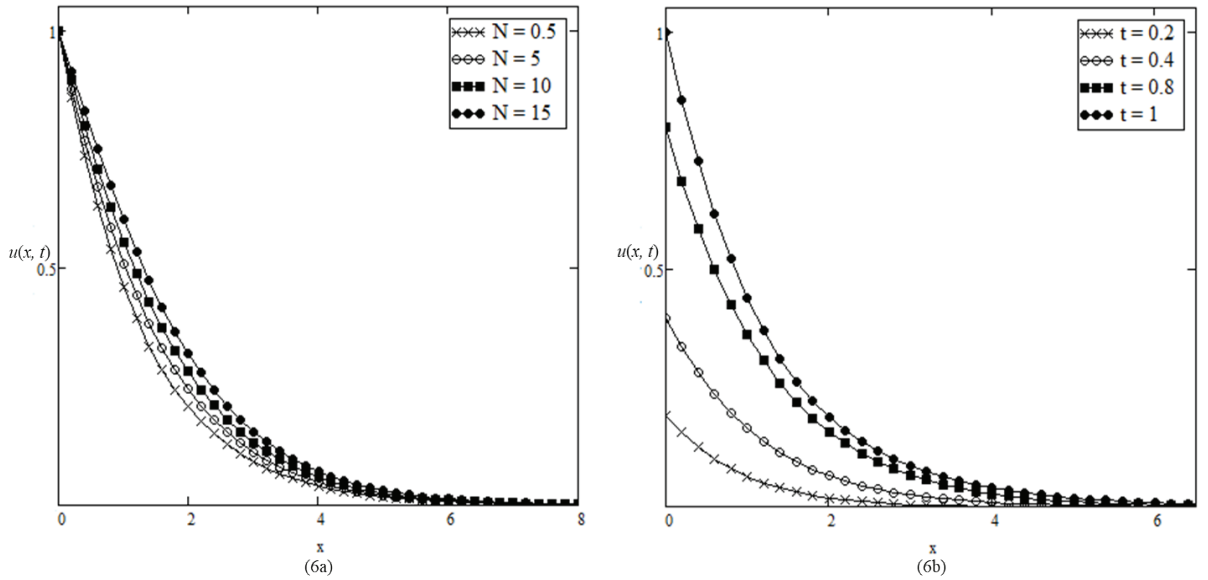

Figure 6. Velocity profiles of different radiation parameter, *N* (6a) and time, *t* (6b).

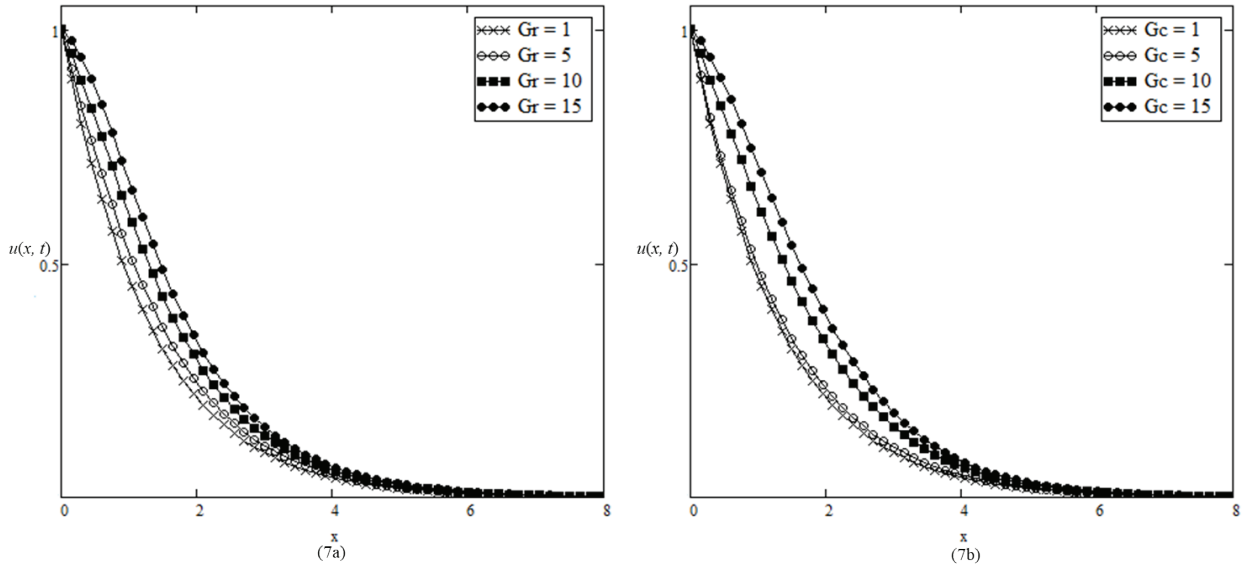

Figure 7. Velocity profiles of different Grashof number, *Gr* (7a) and Grashof concentration number, *Gc* (7b).

prevails over viscous force, complicating the flow dynamics due to its coupling with mass and thermal aspects.

CONCLUSION

The study establishes a mathematical solution for the influence of the Casson fluid parameter on MHD convective heat and mass transfer over an accelerating plate in a porous medium. Important considerations, such as the impact of chemical reactions and radiation, are analysed. The results, obtained through Laplace transform techniques, are acceptable and provide insights into fluid behaviour under the considered conditions. The study's findings have practical implications for applications within engineering and technology fields. In summary, we observed that:

- It is observed that increasing the *Sc* number leads to a reduction in the concentration profile.
- Temperature progressively increases with rising time, *t*.
- An increase in the *Pr* number leads to a decrease in temperature.
- An increase in the radiation constraint, *N* results in a reduction in both the thermal boundary layer thickness and the temperature profile.
- The trend indicates that an increase in the Casson parameter, γ reduces the fluid velocity.
- The velocity is observed to decrease with an increase in magnetic field strength, *M*.
- The velocity increases notably with higher values of the chemical reaction coefficient, *Kr*.
- The velocity decreases in the presence of thermal radiation, *N*.
- The fluid velocity increases over time, *t*.
- A steady elevation in velocity is noticed with the increasing Grashof number, *Gr*.
- An increase in the *Gc* number indicates that species buoyancy force dominates over the viscous hydrodynamic force, resulting in a substantial increase in velocity for Casson fluid.

NOMENCLATURE, SYMBOL AND SUBSCRIPT

γ	Casson parameter fluid in the x – direction
x	fluid in the x – direction
t	Time (s)
u'	velocity (ms^{-1})
T'	temperature (K)
C'	concentration ($molL^{-1}$)
ρ	fluid density (kgm^{-3})
μ	Dynamic viscosity ($kgm^{-1}\,s^{-1}$)
g	acceleration due to gravity (ms^{-2})
β	thermal expansion ($1\,/\,K$)
σ	electrical conductivity ($S\,/\,m$)
B_0	Magnetic field ($Nm^{-1}A^{-1}$)
k	thermal conductivity ($Wm^{-1}K^{-1}$)
φ	porosity of medium
K	permeability of medium (m^2)
c_p	specific heat at constant pressure ($Jkg^{-1}K^{-1}$)
q_r	radiative heat flux (Wm^{-2})
D	mass diffusion (m^{-3})
Kr	chemical reaction parameter (s^{-1})
Pr	Prantl number
Sc	Schmidt number
Gr	Grashof number
Gc	Grashof concentration number

ACKNOWLEDGEMENT

The authors express their gratitude to Ministry of Higher Education Malaysia for supporting this work through the Fundamental Research Grant Scheme, referenced as FRGS/1/2024/STG06/UMP/02/9 (Universiti Malaysia Pahang Al-Sultan Abdullah reference: RDU240132).

AUTHORSHIP CONTRIBUTIONS

Authors equally contributed to this work.

DATA AVAILABILITY STATEMENT

The authors confirm that the data that supports the findings of this study are available within the article. Raw data that support the finding of this study are available from the corresponding author, upon reasonable request.

CONFLICT OF INTEREST

The author declared no potential conflicts of interest with respect to the research, authorship, and/or publication of this article.

ETHICS

There are no ethical issues with the publication of this manuscript.

STATEMENT ON THE USE OF ARTIFICIAL INTELLIGENCE

Artificial intelligence was not used in the preparation of the article.

REFERENCES

[1] Kodi R, Mopuri O, Sree S, Konduru V. Investigation of MHD Casson fluid flow past a vertical porous plate under the influence of thermal diffusion and chemical reaction. Heat Transf 2022;51:377–394. [CrossRef]

[2] Li S, Raghunath K, Alfaleh A, Ali F, Zaib A, Khan MI, et al. Effects of activation energy and chemical reaction on unsteady MHD dissipative Darcy–Forchheimer squeezed flow of Casson fluid over horizontal channel. Sci Rep 2023;13:2666. [CrossRef]

[3] Sulochana C, Aparna SR, Sandeep N. Heat and mass transfer of magnetohydrodynamic Casson fluid flow over a wedge with thermal radiation and chemical reaction. Heat Transf 2021;50:3704–3721. [CrossRef]

[4] Sene N. Solution procedure for fractional Casson fluid model considered with heat generation and chemical Reaction. Sustainability 2023;15:5306. [CrossRef]

[5] Kumar MA, Reddy YD, Goud BS, Rao VS. An impact on non-Newtonian free convective MHD Casson fluid flow past a vertical porous plate the existence of Soret, Dufour, and chemical reaction. Int J Ambient Energy 2022;43:7410–7418. [CrossRef]

[6] Akaje TW, Olajuwon BI, Raj MT. Computational analysis of the heat and mass transfer in a casson nanofluid with a variable inclined magnetic field. Sigma J Eng Nat Sci 2023;41:512–523. [CrossRef]

[7] Osman HI, Vieru D, Ismail Z. Transient Axisymmetric Flows of Casson Fluids with Generalized Cattaneo's Law over a Vertical Cylinder. Symmetry 2022;14:1–14. [CrossRef]

[8] Hussanan A, Aman S, Ismail Z, Salleh MZ, Widodo B. Unsteady natural convection of sodium alginate viscoplastic casson based based nanofluid flow over a vertical plate with leading edge accretion/ablation. J Adv Res Fluid Mech Therm Sci 2018;45:92–98.

[9] Aman S, Zokri SM, Ismail Z, Salleh MZ, Khan I. Casson model of MHD flow of SA-based hybrid nanofluid using Caputo time-fractional models. Defect Diffus Forum 2019;390:83–90. [CrossRef]

[10] Mittal AS, Patel HR. Influence of thermophoresis and Brownian motion on mixed convection two dimensional MHD Casson fluid flow with non-linear radiation and heat generation. Physica A Stat Mech Appl 2020;537:122710. [CrossRef]

[11] Shahrim MN, Mohamad AQ, Jiann LY, Zakaria MN, Shafie S, Ismail Z, et al. Exact solution of fractional convective Casson fluid through an accelerated plate. CFD Letters 2021;13:15–25. [CrossRef]

[12] Hafez NM, Abd-Alla AM, Metwaly TMN. Influences of rotation and mass and heat transfer on MHD peristaltic transport of Casson fluid through inclined plane. Alex Eng J 2023;68:665–692. [CrossRef]

[13] Gholinia M, Javadi H, Gatabi A, Khodabakhshi A, Ganji DD. Analytical study of a two-phase revolving system of nanofluid flow in the presence of a magnetic field to improve heat transfer. Sigma J Eng Nat Sci 2019;37:341–360.

[14] Kodi R, Mopuri O. Unsteady MHD oscillatory Casson fluid flow past an inclined vertical Porous plate in the presence of chemical reaction with heat absorption and Soret effects. Heat Transf 2022;51733–752. [CrossRef]

[15] Ismail Z, Hussanan A, Khan I, Shafie S. MHD and radiation effects on natural convection flow in a porous medium past an infinite inclined plate with ramped wall temperature: An exact analysis. Int J Appl Math and Stat 2013;45:77–86.

[16] Prasad KV, Vajravelu K, Vaidya H, Basha NZ, Umesh V. Thermal and species concentration of MHD Casson fluid at a vertical sheet in the presence variable fluid properties. Ain Shams Eng J 2018;9:1763–1779. [CrossRef]

[17] Jagadesh V, Sreenadh S, Ajithkumar M, Lakshminarayana P, Lakshminarayana P, Sucharitha G. Investigation of dissipative heat transfer and peristaltic pumping on MHD Casson fluid flow in an inclined channel filled with porous medium. Numer Heat Trans B Fund 2023;85:1654–1672. [CrossRef]

[18] Raza J, Oudina FM, Ali H, Sarris IE. Slip effects on Casson nanofluid over a stretching sheet with activation energy: RSM analysis. Front Heat Mass Transf 2024;22:1017–1041. [CrossRef]

[19] Dharmaiah G, Oudina FM, Balamurugan KS, Vedavathi N. Numerical analysis of the magnetic dipole effect on a radiative ferromagnetic liquid flowing over a porous stretched sheet. Fluid Dyn Mater Process 2023;20:293–310. [CrossRef]

[20] Kataria HR, Patel HR. Radiation and chemical reaction effects on MHD Casson fluid flow past an oscillating vertical plate embedded in porous medium. Alex Eng J 2016;55:583–595. [CrossRef]

[21] Akinbo BJ, Olajuwon BI. Heat and mass transfer in Magnetohydrodynamics (MHD) flow over a moving vertical plate with convective boundary condition in the presence of thermal radiation. Sigma J Eng Nat Sci 2019;37:1031–1053.

[22] Omar NFM, Osman HI, Mohamad AQ, Jusoh R, Ismail Z. Effects of Radiation and Magnetohydrodynamic on Unsteady Casson Fluid Over Accelerated Plate. J Adv Res Fluid Mech Therm Sci 2021;85:93–100. [CrossRef]

[23] Khan H, Qayyum M, Khan O, Ali M. Unsteady squeezing flow of Casson fluid with magnetohydrodynamic effect and passing through porous medium. Math Probl Eng 2016;2016:4293721. [CrossRef]

[24] Khan D, Khan A, Khan I, Ali F, Karim F, Tlili I. Effects of relative magnetic field, chemical reaction, heat generation and Newtonian heating on convection flow of Casson fluid over a moving vertical plate embedded in a porous medium. Sci Rep 2019;9:400. [CrossRef]

[25] Goud BS, Kumar PP, Malga BS. Effect of heat source on an unsteady MHD free convection flow of Casson fluid past a vertical oscillating plate in porous medium using finite element analysis. Partial Differ Equ Appl Math 2020;2:100015. [CrossRef]

[26] Jalili P, Azar AA, Jalili B, Ganji DD. Study of nonlinear radiative heat transfer with magnetic field for non-Newtonian Casson fluid flow in a porous medium. Results Phys 2023;48:106371. [CrossRef]

[27] Vera MR, Niño Y, Valencia A. On the application of the fourier series solution to the hydromagnetic buoyant two-dimensional laminar vertical jet. Math Probl Eng 2012;2012:986834. [CrossRef]

[28] Kumar KL. Engineering Fluid Mechanics. 8th Ed. New Delhi: S. Chand; 2014.

[29] Kumar DS. Fluid Mechanics and Fluid Power Engineering. 8th ed. New Delhi: Katson Books; 2013.

[30] Modi PN, Seth SM. Hydraulics & Fluid Mechanics Including Hydraulics Machines. 19th ed. New Delhi: Standard Book House; 2017.

[31] Manshoor B, Khalid A, Sapit A, Zaman I, Mohammad AN. Numerical solution of Burger's equation based on Lax-Friedrichs and Lax-Wendroff schemes. AIP Conf Proc 2017;1831. [CrossRef]

[32] Egbako UA, Adeboye KR. One-Step, Sixth Order Numerical Method via Pade Approximations for the Solutions of Stiff Differential Equations. Am J Comput Appl Math 2012;2:10–13. [CrossRef]

[33] Nazri NN, Manshoor B, Zaman I, Didane DH, Abdelaal MAS, Ibrahim MN. Velocity and shear stress distribution of laminar flow between parallel plate by laplace transform approach. J Complex Flow 2022;4:19–23.

[34] Seilabi SE. Dimensional analysis and analytical solutions. In: El-Amin MF, editors. Numerical Modeling of Nanoparticle Transport in Porous Media. 1st ed. Amsterdam: Elsevier; 2023. p. 33–56.

[35] Woodbury KA, Najafi H, Monte F, Beck JV. Inverse Heat Conduction: Ill-Posed Problems. 2nd ed. New Jerjey: Wiley; 2023.

[36] Kucheva NA. Analytical solution of the problem of thermoelasticity for a plate heated by a source with a constant heat supply on one surface. Turk J Comput Math Educ 2021;12:1622–1633.

[37] Kato S, Matsuda S. Analytical solution for the problem of one-dimensional quasi-steady non-charring ablation in a semi-infinite solid with temperature-dependent thermo-physical properties. Therm Sci Eng Prog 2022;3:101181. [CrossRef]

[38] Noranuar WNN, Mohamad AQ, Lim YJ, Shafie S. Analytical Simulation of Magnetohydrodynamics Casson Blood Flow using Carbon Nanotubes in a Channel with Atherosclerosis Condition. Semarak Current Biomedical Res J 2024;1:1–17. [CrossRef]